Research article

Embedding CeO$_2$ nanocontainers in a TiO$_2$ coating on glass surfaces

Jacinthe Gagnon [1,2,*], Rachel A. Caruso [2], and Katharina M. Fromm [1,*]

[1] Department of Chemistry and Fribourg Center for Nanomaterials, University of Fribourg, Chemin du Musée 9, 1700 Fribourg, Switzerland
[2] PFPC, School of Chemistry, The University of Melbourne, Melbourne, Victoria 3010, Australia

* Correspondence: Email: jacinthe.gagnon@iaf.inrs.ca; katharina.fromm@unifr.ch.

Abstract: Various strategies are being developed for the prevention of implant-related infections. One of them is the encapsulation of antimicrobial drugs in inorganic containers that can be released at the site of the implant. However, the attachment of such containers onto implant surfaces may be a challenge. In this study, it is demonstrated that CeO$_2$ nanocontainers can be added to a TiO$_2$ coating on glass surfaces. The structure, crystal phase and surface properties of the nanocontainers were characterized by transmission electron microscopy, scanning electron microscopy (SEM), powder X-ray diffraction, infrared spectroscopy, Raman spectroscopy and a zetasizer. The coatings were analyzed by SEM and energy-dispersive X-ray spectroscopy to determine their homogeneity and ensure CeO$_2$ encapsulation. The coatings were stable in air over prolonged time periods (> 6 months) and therefore hold promise for pursuing in biomedical applications.

Keywords: nanocontainers; ceria; titania; coating; biomaterials

1. Introduction

Orthopedic implants are nowadays routinely used in medicine. There is a huge variety of implants, with bone implants being the most used [1]. Metal-based materials are commonly used for load-bearing bone and tooth replacement applications because of their good mechanical properties (strength, elasticity, corrosion resistance and fracture toughness) and low toxicity [2]. Titanium-based materials and titanium alloys are commonly applied due to their good corrosion resistance, their excellent hard-tissue biocompatibility and their ability for enhancing osseointegration, i.e. their ability to promote bone growth on a material surface [3,4]. It is well

known that titanium is covered with a thin layer of TiO_2 in aqueous solutions [5], therefore considerable attention has been placed on titania coatings because of the success of titanium implants.

Implant-related infections still remain an issue, and various strategies, such as the use of silver-containing materials, are currently under development in order to prevent them [6]. Ceria (CeO_2) is a good candidate for biomedical applications as it has low toxicity and potential protective properties against oxidative stress [7]. We have recently demonstrated that ceria nanocontainers are promising candidates as silver-drug carriers [8,9]; such nanocontainers could have potential for the prevention of implant-related infections. The silver nanoparticles (AgNPs) could be encapsulated in the CeO_2 nanocontainers by incorporating them during the nanocontainer synthesis. Silver nitrate ($AgNO_3$) can be encapsulated within the nanocontainers via a soaking method [8]; this method could be used for a variety of other compounds (it was previously demonstrated for encapsulating anti-corrosive agents [10,11]). We have also demonstrated that a TiO_2 coating around silver-containing CeO_2 nanocontainers can protect against uncontrolled silver release [9]. However, the issue of how to attach these nanocontainers on to surfaces needs to be resolved. In the case of implants, coatings should be well adhered to the surface in order to prevent the release of undesirable particles into the surrounding tissues, which often cause inflammatory responses and is one of the major causes of implant failure [12,13].

One strategy to coat a biomaterial with nanoparticles is to incorporate these nanoparticles either within a coating or in the biomaterial itself during their synthesis. This therefore enables the trapping of the nanoparticles within the material network. As an example, Fe_3O_4 nanoparticles were embedded in a polyurethane matrix. The nanoparticles were retained and stabilized in the matrix structure rather than being retained by the electrostatic interactions of the inorganic nanoparticles with the hyperbranched and highly functionalized matrix [14].

The use of TiO_2 thin films to encapsulate silver drugs was already suggested for biomedical implant applications [15,16]. Song et al. [16] demonstrated that these coatings could embed AgNPs and release silver continuously over a 30 h period, while demonstrating no cytotoxicity via a 3-(4,5-dimethylthiazol-2-yl)-2,5-diphenyltetrazolium bromide (MTT) assay.

The dip-coating method has been previously demonstrated successful for the immobilization of CeO_2 NPs on silk fibers, thus improving the UV-protection and antibacterial properties of silk [17]. In the present study, a similar strategy to trap ceria nanocontainers within a titania coating is presented. In this case, glass was used as the substrate because its surface can be easily modified and it has good biocompatibility [18,19].

2. Experimental Methods

2.1. Reagents

All chemicals and solvents were purchased from Sigma-Aldrich unless otherwise stated, were of the highest quality available and were used without any further purification, except for styrene that was distilled twice before use. The polyvinylpyrrolidone (PVP) had an average molecular weight of 40,000 g/mol. Microscope glass slides for surface coating experiments were provided by Yancheng Huida Medical Instruments Co., China and their composition was 72.00% SiO_2, 14.50% Na_2O, 7.05% CaO, 3.95% MgO, 1.65% Al_2O_3, 0.30% K_2O, and 0.06% Fe_2O_3.

2.2. Synthesis of CeO₂ nanocontainers

CeO$_2$ nanocontainers were synthesized as previously described [8,9,20]. First, the polystyrene (PS) template was prepared by adding doubly-distillated styrene (3.70 g, 35.5 mmol), potassium persulfate (KPS, 0.30 g, 1.1 mmol), and sodium dodecyl sulfate (SDS, 0.09 g, 0.3 mmol) to water (250 ml). The reaction mixture was heated at 80 °C under argon with constant stirring for 40 h. The PS beads were washed three times by centrifugation at 15,000 rpm for 30 min and were resuspended in 5 ml water. Then 1 ml of the PS mixture was mixed with cerium acetyl acetonate (Ce(acac)$_3$, 0.70 g, 1.6 mmol), polyvinylpyrrolidone (PVP, 0.30 g, 0.0075 mmol) and urea (0.30 g, 5.0 mmol) in 40 ml water. The solution was then aged at 100 °C for 4 to 5 days. The coated beads were washed three times with water by centrifugation at 15,000 rpm for 30 min and dried at 40 °C. Hollow CeO$_2$ nanocontainers were obtained after calcination in air at 600 °C for 4 h.

2.3. Entrapment of CeO₂ nanocontainers in TiO₂ coating on glass

First the sol solution was prepared in a plastic bottle. The sol consisted of 17 ml of titanium butoxide (17.00 g, 50.0 mmol) dissolved in 35 ml of acetyl acetone in butanol solution (7.8 ml of acetyl acetone in 96.0 ml of 1-butanol). The CeO$_2$ nanocontainers (0.10 g) were then added to the sol (for the glass slide covered with only TiO$_2$, the CeO$_2$ nanocontainers were omitted). The reaction flask was covered with parafilm and was stirred for 1 h. Afterwards, 15 ml of water in a propanol solution (11.0 ml of Milli-Q water in 34.5 ml of isopropanol) was rapidly added. The flask was covered with parafilm and the solution was stirred for 1 h. Then 2.0 ml of acetonitrile was added to the solution. The flask was covered again with parafilm and stirred for 1 h. The stirring was then stopped and the solution was aged overnight at room temperature. Note that parafilm (Parafilm® M) was used to seal the flask. This parafilm is resistant to water and alcohols [21]. Although resistance of Parafilm® M to acetyl acetone and acetonitrile was not determined, the parafilm did not show any sign of deterioration and never came into direct contact with the solutions, hence parafilm contamination of the solution or sample is considered negligible.

The glass slide was cleaned immediately prior to coating by immersing in Milli-Q water and sonicating for 10 min. It was then immersed in isopropanol, sonicated for another 10 min and then rinsed once with isopropanol and dried in air for 2 to 3 h. The glass slide was placed flat at the bottom of a plastic bottle. The sol solution was stirred for one minute to resuspend the CeO$_2$ nanocontainers and then poured in to the bottle containing the glass slide. The sol was aged for 1 h, which allowed the nanocontainers to deposit on the glass slides. The slide was then slowly dragged out of the sol over a period of approximately 30 sec at an angle of about 60° compared to the horizontal position and dried in a horizontal position at room temperature overnight. The following day, the glass slide was calcined at 500 °C for 2 h with air flow.

2.4. Characterization

Transmission electron microscopy (TEM, FEI Tecnai F20 microscope) and scanning electron microscopy (SEM, high-resolution field emission environmental SEM Quanta 200 FEI equipped with an energy-dispersive X-ray spectroscopy (EDS) detector) were used to characterize the morphology of the synthesized nanocontainers and the coating surfaces. A HORIBA LabRAM HR

Raman confocal microspectrometer was used for Raman spectroscopy and Fourier transform infrared (FTIR) spectra were obtained using a Bruker Tensor 27 FTIR equipped with a MKII Golden Gate Single Attenuated Total Reflection System. The zeta-potential was measured in water at pH 6.5 using a Zetasizer 2000 from Malvern.

3.   Results and Discussion

CeO$_2$ nanocontainers were synthesized as previously described [8,9,10]. The spherical shape and hollow nature of the nanocontainers was confirmed by SEM (Figure 1A) and TEM (Figure 1B). The PXRD pattern gave peak intensities corresponding to the fluorite crystalline phase of CeO$_2$ (JCPS No. 34-0394, Figure 1C).
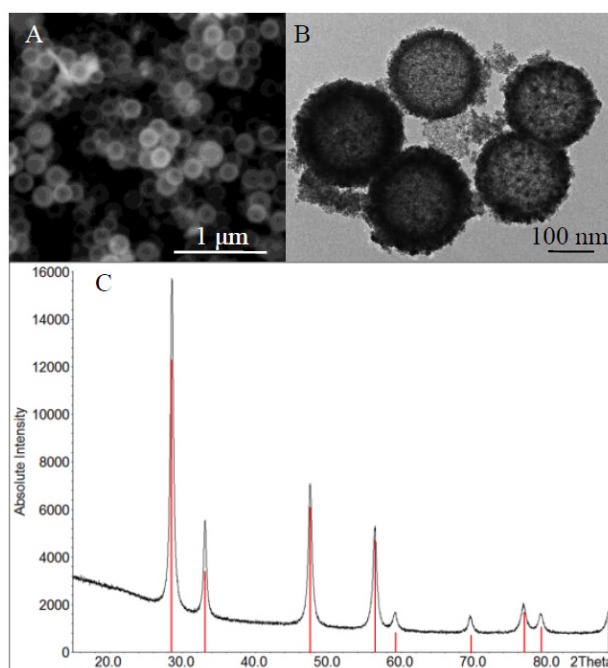

Figure 1. SEM (A) and TEM (B) images and PXRD pattern (C) of the CeO$_2$ nanocontainers. The red lines in the XRD pattern (C) correspond to the theoretical peak positions of fluorite crystalline CeO$_2$ phase (JCPS No. 34-0394).

One approach to attach these nanocontainers on a surface is using covalent bonds as CeO$_2$ materials are often functionalized by covalent modification via the hydroxyl groups normally present on the CeO$_2$ surface [22,23,24]. However, as can be observed from the FT-IR spectrum of the ceria nanocontainers shown in Figure S1A, there are no detectable hydroxyl groups, despite the CeO$_2$ nanocontainers being negatively charged (Figure S2). This surprising result was further confirmed by Raman spectroscopy, where again no hydroxyl groups were indicated (Figure S1B). The intense band at 462 cm^{-1} in the Raman spectrum is attributed to the Ce-O stretching vibrations [25].

Another strategy to attach particles with low reactivity is to embed them into a matrix. In order to do so, CeO$_2$ nanocontainers were added to a titanium butoxide sol, which was then used to coat a glass slide. The method is depicted in Figure S3. The resulting coatings are easily observed with the naked eye, as shown in Figure 2. Before coating, the glass slide is colorless (Figure 2A). When it is

coated with TiO_2 only, the slide is covered with a thin white film (Figure 2B). The rough appearance of the surface is due to an uneven TiO_2 thickness over the glass surface. When the glass slide is covered with the CeO_2 nanocontainers and TiO_2 film, the surface becomes rougher because of the CeO_2 particles (Figure 2C). Note the CeO_2 sample is pale yellow in color, making the film yellowish. The nanocontainers are entrapped in the TiO_2 film and do not fall off the glass slide. The coating remained intact, as observed visually, for prolonged time periods (at least 6 months) in air, even though they were not protected from light. This would indicate that the nanocontainers are within the TiO_2 network on the glass substrate.
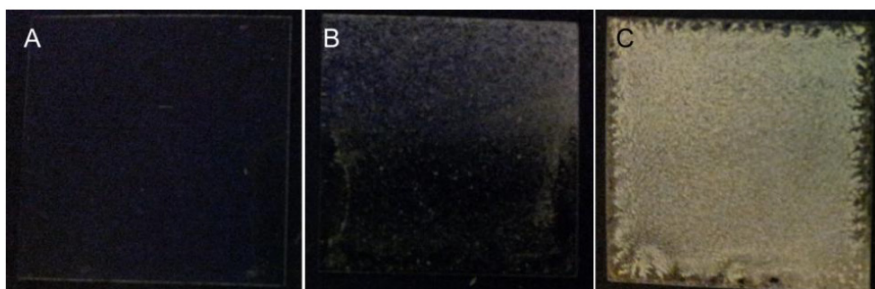

Figure 2. Photographs of glass coverslips before (A) and after coating with TiO_2 only (B) and after coating with CeO_2 nanocontainers in a TiO_2 film (C). The dimensions of the coverslips are 22 mm × 22 mm.

In order to confirm the presence of the CeO_2 nanocontainers and TiO_2 film on the glass substrate, SEM and EDS were performed. The results from the EDS analyses are tabulated in the supplementary materials (Tables S1, S2 and S3). As controls, half of a glass slide was coated only with TiO_2, while another half remained uncoated. The side with bare glass was mainly composed of oxygen, silicon, sodium, magnesium, aluminum and potassium, as specified by the provider. This was confirmed from the EDS data (Figure 3A and Table S1).

When the glass slide was coated only with TiO_2, titanium appears as the main component of the slide after oxygen (Figure 3B). As one can see from the SEM image (Figure 3B-inset), the TiO_2 layer tends to form cracks, probably during the drying. Despite this, the TiO_2 film covers the whole glass surface that was dipped into the titanium butoxide sol.

When the glass slide was coated with the CeO_2 nanocontainers entrapped within the TiO_2 film, the CeO_2 nanocontainers are apparent in the SEM image (Figure 3C-inset). However, the nanocontainers are not homogeneously dispersed throughout the film and tend to be present in aggregates. From the EDS, one can observe that cerium became the main component per weight, followed by oxygen, silicon and titanium. While an even dispersion has not been obtained, this approach appears sufficient to embed the nanocontainers within the TiO_2 coating. The CeO_2 nanocontainer and TiO_2 coating also forms cracks upon drying (data not shown).

These results show promise for embedding particles into a coating. Karakoti et al. [26] have successfully entrapped ceria nanoparticles within a bioactive glass and showed that the addition of ceria nanoparticles did not induce any cytotoxicity to cells, but they promoted osteoblastic differentiation, making this new bioactive glass interesting for bone regeneration applications. More recently, Catauro et al. [27] have demonstrated that TiO_2-based coatings could improve the biocompatibility of titanium implants. As the ceria nanocontainers have been shown to encapsulate

silver nanoparticles, this titania coating containing ceria could be further developed and studied for silver release.
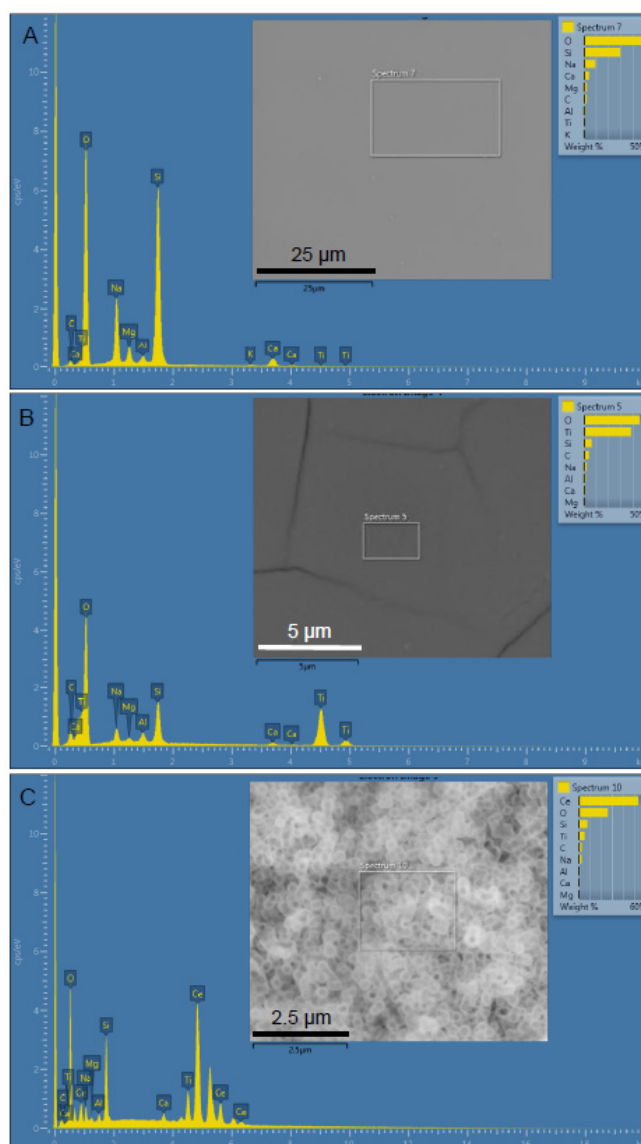

Figure 3. EDS and SEM images (inset) of an uncoated glass slide (A), a glass slide coated with TiO_2 film (B) and a glass slide coated with CeO_2 nanocontainers and TiO_2 film (C).

4. Conclusion

Glass surfaces were coated with TiO_2 and this coating could be embedded with CeO_2 nanocontainers when they were added to the titanium-based sol prior to film formation. Improvements in the approach are required in order to reduce cracking in the TiO_2 film and to better distribute the nanocontainers. The homogeneity of the film could possibly be achieved using a spin coater. Future work would include scratch tests on the coatings, release experiments and biocompatibility tests. This article demonstrates that CeO_2 nanocontainers can be embedded in TiO_2

coatings despite the low CeO_2 reactivity. This method holds promise for future research on implant coatings.

Acknowledgements

This paper is dedicated to Prof. Eva-Marie Hey-Hawkins on behalf of her 60th birthday.

Conflict of Interest

The authors declare no conflicts of interest in this paper.

References

1. Jagur-Grodzinski J (2006) Polymers for tissue engineering, medical devices, and regenerative medicine. Concise general review of recent studies. *Polym Advan Technol* 17: 395–483.
2. Hanawa T (2012) Research and development of metals for medical devices based on clinical needs. *Sci Technol Adv Mater* 13: 064102–064116.
3. Ellingsen JE, Lyngstadaas SP (2003) Bio-implant interface: improving biomaterials and tissue reactions. CRC Press.
4. Minagar S, Wang J, Berndt CC, et al. (2013) Cell response of anodized nanotubes on titanium and titanium alloys. *J Biomed Mater Res* 101A: 2726–2739.
5. Effah EAB, Bianco PD, Ducheyne P (1995) Crystal-structure of the surface oxide layer on titanium and its changes arising from immersion. *J Biomed Mater Res* 29: 73–80.
6. Eckhardt S, Brunetto PS, Gagnon J, et al. (2013) Nanobio silver: its interactions with peptides and bacteria, and its uses in medicine. *Chem Rev* 113: 4708–4754.
7. Gagnon J, Fromm KM (2015) Toxicity and protective effects of cerium oxide nanoparticles (nanoceria) depending on their preparation method, particle size, cell type, and exposure route. *Eur J Inorg Chem* 2015: 4510–4517.
8. Gagnon J, Clift MJD, Vanhecke D, et al. (2015) Integrating silver compounds and nanoparticles into ceria nanocontainers for antimicrobial applications. *J Mater Chem B* 3: 1760–1768.
9. Gagnon J, Clift MJD, Vanhecke D, et al. (2016) Synthesis, characterization, antibacterial activity and cytotoxicity of hollow TiO_2-coated CeO_2 nanocontainers encapsulating silver nanoparticles for controlled silver release. *J Mater Chem B* 4: 1166–1174.
10. Kartsonakis I, Daniilidis I, Kordas G (2008) Encapsulation of the corrosion inhibitor 8-hydroxyquinoline into ceria nanocontainers. *J Sol-Gel Sci Techn* 48: 24–31.
11. Borisova D, Akçakayıran D, Schenderlein M, et al. (2013) Nanocontainer-based anticorrosive coatings: effect of the container size on the self-healing performance. *Adv Funct Mater* 23: 3799–3812.

12. Jiang Y, Jia T, Wooley PH, et al. (2013) Current research in the phathogenesis of aseptic implant loosening associated with particulate wear debris. *Acta Orthop Belg* 79: 1–9.

13. Wooley PH, Morren R, Andary S, et al. (2002) Inflammatory responses to orthopaedic biomaterials in the murine air pouch. *Biomaterials* 23: 517–526.

14. Das B, Mandal M, Upadhyay A, et al. (2013) Bio-based hyperbranched polyurethane/Fe_3O_4 nanocomposites: smart antibacterial biomaterials for biomedical devices and implants. *Biomed Mater* 8: 035003–035014.

15. Lorenzetti M, Biglino D, Novak S, et al. (2014) Photoinduced properties of nanocrystalline TiO_2-anatase coating on Ti-based bone implants. *Mater Sci Eng C* 37: 390–398.

16. Song DH, Uhm SH, Kim SE, et al. (2012) Synthesis of titanium oxide thin films containing antibacterial silver nanoparticles by a reactive magnetron co-sputtering system for application in biomedical implants. *Mater Res Bull* 47: 2994–2998.

17. Lu Z, Mao C, Meng M, et al. (2014) Fabrication of CeO_2 nanoparticle-modified silk for UV protection and antibacterial applications. *J Colloid Interf Sci* 435: 8–14.

18. Brook IM, Hatton PV (1998) Glass-ionomers: bioactive implant materials. *Biomaterials* 19: 565–571.

19. Hum JH, Boccaccini AR (2012) Bioactive glasses as carriers for bioactive molecules and therapeutic drugs: a review. *J Mater Sci Mater Med* 23: 2317–2333.

20. Kartsonakis IA, Liatsi P, Daniilidis I, et al. (2008) Synthesis, characterization, and antibacterial action of hollow ceria nanospheres with/without a conductive polymer coating. *J Am Ceram Soc* 91: 372–378.

21. http://www.sigmaaldrich.com/catalog/product/sigma/p7793?lang=fr&region=CA&gclid=Cj0KE QiAnvfDBRCXrabLl6-6t-0BEiQAW4SRUPVOSTgTtcJTSasj1ZiSmi0B0EFT5mldnbgH-N0yw zUaAly38P8HAQ).

22. Sun L, Huang C, Gong T, et al. (2010) A biocompatible approach to surface modification: biodegradable polymer functionalized super-paramagnetic iron oxide nanoparticles. *Mater Sci Eng C* 30: 583–589.

23. Zhang ZF, Yu L, Liu W, et al. (2010) Surface modification of ceria nanoparticles and their chemical mechanical polishing behavior on glass substrate. *Appl Surf Sci* 256: 3856–3861.

24. Sahu SK, Chakrabarty A, Bhattacharya D, et al. (2011) Single step surface modification of highly stable magnetic nanoparticles for purification of his-tag proteins. *J Nanopart Res* 13: 2475–2484.

25. Kosacki I, Suzuki T, Anderson HU, et al. (2002) Raman scattering and lattice defects in nanocrystalline CeO_2 thin films. *Solid State Ionics* 149: 99–105.

26. Karakoti AS, Tsigkou O, Yue S, et al. (2010) Rare earth oxides as nanoadditives in 3-D nanocomposite scaffolds for bone regeneration. *J Mater Chem* 20: 8912–8919.

27. Catauro M, Papale F, Bollino F (2015) Characterization and biological properties of TiO_2/PCL hybrid layers prepared via sol-gel dip coating for surface modification of titanium implants. *J Non-Cryst Solids* 415: 9–15.